




Synthesis, structure, computational, antimicrobial and in vitro anticancer studies of copper(II) complexes with N,N,N',N'-tetrakis(2-hydroxyethyl)ethylenediamine and tris(2-hydroxyethyl)amine

R. Kumar, S. Obrai, A.K. Jassal, M.S. Hundal, J. Mitra & S. Sharma


To cite this article: R. Kumar, S. Obrai, A.K. Jassal, M.S. Hundal, J. Mitra & S. Sharma (2015) Synthesis, structure, computational, antimicrobial and in vitro anticancer studies of copper(II) complexes with N,N,N',N'-tetrakis(2-hydroxyethyl)ethylenediamine and tris(2-hydroxyethyl)amine, *Journal of Coordination Chemistry*, 68:12, 2130-2146, DOI: [10.1080/00958972.2015.1031120](https://doi.org/10.1080/00958972.2015.1031120)


To link to this article: <http://dx.doi.org/10.1080/00958972.2015.1031120>

 View supplementary material 

 Accepted author version posted online: 19 Mar 2015.
Published online: 21 Apr 2015.

 Submit your article to this journal 

 Article views: 135

 View related articles 

 View Crossmark data 

Synthesis, structure, computational, antimicrobial and *in vitro* anticancer studies of copper(II) complexes with N,N,N',N'-tetrakis(2-hydroxyethyl)ethylenediamine and tris(2-hydroxyethyl)amine

R. KUMAR*^{†,1}, S. OBRAI*[†], A.K. JASSAL[‡], M.S. HUNDAL[‡], J. MITRA[§] and S. SHARMA[¶]

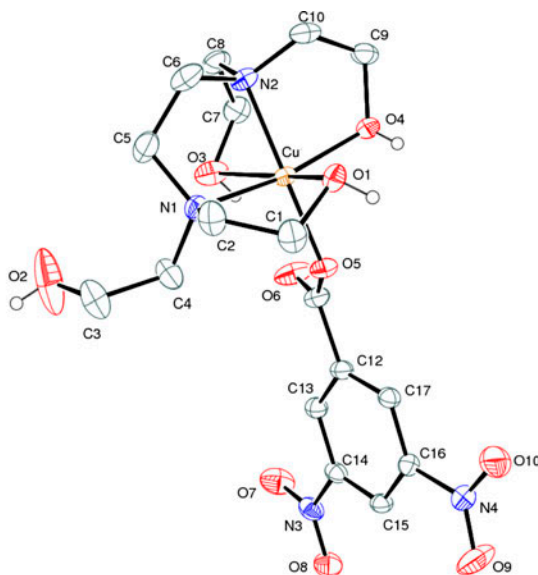
[†]Department of Chemistry, Dr. B. R. Ambedkar National Institute of Technology, Jalandhar, India

[‡]Department of Chemistry, Guru Nanak Dev University, Amritsar, India

[§]Discipline of Inorganic and Materials Catalysis, CSIR-CSMCRI, Bhavnagar, India

[¶]Department of Biotechnology & Microbiology, Arni School of Basic Sciences, Arni University, Indora, India

(Received 2 September 2014; accepted 4 March 2015)



The present work consists of synthesis, crystal structure, DFT studies, antimicrobial, and anticancer activities of [Cu(THEEN)(DNB)](DNB) (**1**) and [Cu(TEAH₃)₂](DNB)₂ (**2**). Both complexes have distorted octahedron geometries with Jahn–Teller distortion. The theoretical and crystallographic analyses are consistent with each other.

*Corresponding authors. Email: rakesh_nitj@yahoo.co.in (R. Kumar); o.sangeeta@yahoo.com (S. Obrai)

¹Present address: Department of Applied Sciences, CTIT, CT Group of Institutions, Jalandhar, India.

The present work consists of synthesis, structural characterization, spectral, density functional theory (DFT), antimicrobial, and anticancer studies of two copper(II) complexes, [Cu(THEEN)(DNB)] (DNB) (**1**) and [Cu(TEAH₃)₂](DNB)₂ (**2**). In these complexes, THEEN is N,N,N',N'-tetrakis(2-hydroxyethyl)ethylenediamine, a tetrapodal ligand, and TEAH₃ is tris(2-hydroxyethyl)amine, a tripodal ligand, and the counter-anion is 3,5-dinitrobenzoate (DNB⁻). X-ray crystallography studies reveal that both complexes have distorted octahedron geometries. DFT studies have been performed to calculate structural parameters, vibrational bands, and energy gaps of frontier orbital (HOMO-LUMO) with B3LYP/6-31G*/LANL2DZ level of theory using DMSO as solvent. The theoretical and crystallographic analyses are consistent. Antimicrobial studies have been performed with new copper(II) complexes against Gram(+) bacteria (*Staphylococcus aureus*), Gram(-) bacteria (*Serratia marcescens*, *Sphingobium japonicum*, and *Stenotrophomonas maltophilia*) and fungal species (*Candida albicans*, *Aspergillus niger*, and *Saccharomyces cerevisiae*). The copper(II) complexes have also shown *in vitro* cytotoxicity on MCF-7, HCT-116, and HL-60 human cell lines. This study demonstrates that **2** was active against MCF-7 cell lines with IC₅₀ of 23 µg/mL.

Keywords: Crystal structure; DFT studies; Jahn-Teller distortion; Hydrogen bonding; HOMO-LUMO; Antimicrobial and anticancer activity

1. Introduction

There is development in the copper coordination chemistry in both biological and non-biological areas [1]. An important biological aspect of copper coordination chemistry is biomimetic coordination, developing models for copper proteins and enzymes [2]. These models have assisted in understanding the relationship between coordination geometry, nature of donors, and redox potentials [3, 4]. Metal-based complexes as anticancer drugs have improved clinical effectiveness, reduced toxicity, and increased effectiveness. Anticancer drugs based on coinage metals are potential candidates to fulfill this requirement. Many platinum-based complexes have been reported, but there is a need to synthesize nonplatinum-based metal complexes with less toxicity and side effects [5]. Although increasing attention has been paid to the design of copper complexes with polydentate ligands as models of copper oxidases and some mononuclear compounds have been recognized as catalysts for alkane oxidation, the use of poly-copper complexes for such reactions still remains unexplored [6]. The complex [Cu(pyrimol)Cl] investigated by density functional theory (DFT) and spectral techniques is a biomimetic model of the enzyme galactose and is capable of oxidation of primary alcohols [7]. Modeling of the active sites in copper proteins like hemocyanin [8] containing a dicopper center was carried out by time-dependent density functional theory [9].

Growth in biological areas is stimulated by the tendency of copper complexes to undergo biochemical reactions through Cu(I)/Cu(II) redox behavior. Copper species are present in many enzymes as di-, tri-, or polynuclear Cu centers that catalyze selectively various oxidation reactions [10]. Copper(I/II) complexes are endowed with medicinal applications especially with antitumor activity. Xu and co-workers described the *in vitro* cytotoxicity of a copper complex, [Cu(Hptc)(Me₂bpy)(H₂O)]·3H₂O (H₃ptc = pyridine-2,4,6-tricarboxylic acid; Me₂bpy = 4,4'-dimethyl-2,2'-dipyridine), on HeLa cell lines, and it was more effective than cisplatin [11]. Copper(II) complexes with heterocyclic ligands also possess strong cytotoxicity against several human alimentary carcinoma cell lines [12]. The *in vitro* cytotoxicity of a copper(II) complex toward cell lines was reported, and such complexes may play an important role in cytotoxic activities [13]. Macrocyclic dicopper(II) complexes have shown cytotoxicity in human cervical HeLa cancer cells lines [14]. Recently, Wani

et al. have reported the moderate cytotoxic activity of a Cu(II) complex based on oxopyrrolidine-based heterocyclic ligand [15]. In the present article, both Cu(II) complexes were assessed for their possible antimicrobial and cytotoxic properties.

Elevated levels of copper have been found in many types of human cancers [16, 17]. In Wilson's disease, copper accumulated mainly in liver and brain [18]. Other important therapeutical uses of copper complexes are as antimicrobial [19, 20], antiviral, and anti-inflammatory agents [21, 22]. From the literature survey, it is clear that copper complexes have higher anticancer, antibacterial, and antibiotic activities with lower toxicity than platinum compounds [22].

Copper complexes derived from copper chloride and crown ethers were extremely efficient catalysts for the aerobic oxidation of unactivated hydrocarbons [23]. Copper triethanolamine complexes possessing dimeric, trimeric, tetrameric, and polymeric structures are selective and active catalysts for the oxidation of alkenes. But tetrameric $[\text{OCCu}_4(\text{tea})_4(\text{BOH})_4][\text{BF}_4]_2$ (where tea is triethanolaminato) exhibited the highest yield among all complexes [24].

In view of the versatile applications of copper complexes in various fields, the present synthesis, spectral and structural characterization, theoretical modeling, and antimicrobial studies of complexes of a tripodand, tris(2-hydroxyethyl)amine (TEAH₃), and a tetrapodand, N,N,N',N'-tetrakis(2-hydroxyethyl)ethylenediamine (THEEN), with copper(II) under the influence of 3,5-dinitrobenzoate anion has been carried out. Recently, we reported the same studies with picrate as a counter-anion [25(a) and (b)]. The counter-anion has a large influence on the coordination modes of the ligand, geometries adopted by the metal ions and other structural parameters of the complexes as shown by the structures here.

2. Experimental

2.1. Materials and instrumentation

All chemicals and solvents were purchased from commercial sources and used as received. THEEN and TEAH₃ were supplied by Sigma Aldrich and used without purification. 3,5-Dinitrobenzoic acid was used without purification. IR spectra were performed using a Perkin Elmer FT-IR RX I spectrometer from 450 to 4000 cm⁻¹ at room temperature using KBr pellets (Sigma Aldrich). IR peaks near 3300–3400 cm⁻¹ may be due to moisture of KBr that is used for carrying out the IR spectrum of **1** and **2**, because there is no water in the complexes. The elemental analyses were performed on a Flash 2000 Organic Elemental Analyzer. UV–vis spectra were recorded on a Shimadzu Pharmaspec UV-1700 UV–vis spectrophotometer in DMSO cuvettes of 1 cm pathlength. The EPR spectra of the copper complexes were obtained on a Varian ESR spectrophotometer using X-band frequency (9.5 GHz) at room temperature. For antimicrobial activity, pathogenic bacteria *Serratia marcescens* (MTCC-97), *Sphingobium japonicum* (MTCC-6362), *Stenotrophomonas maltophilia* (MTCC-2446), and *Staphylococcus aureus* (MTCC-3160) were procured from the Microbial Type Culture Collection (MTCC), Institute of Microbial Technology, Chandigarh, India. For anticancer activities, MEM RPMI-1640, 3-(4,5-methylthiazole-2-yl)-2,5-diphenyltetrazolium bromide (MTT), penicillin, streptomycin, L-glutamine, pyruvic acid, trypsin/EDTA solution, and fetal bovine serum (FBS) were purchased from Sigma Chemical Co., St. Louis, MO (USA). All other reagents used were AR grade and available locally.

2.2. X-ray crystallography

X-ray crystallographic measurements for **1** and **2** were carried out on a Bruker APEX-II CCD area detector diffractometer with graphite-monochromated Mo K α ($\lambda = 0.71073$ Å) radiation. The crystal structures were solved by direct methods using the program SIR-97 [26] and refined with full-matrix least-squares methods on F^2 using SHELXL-97 [27]. Absorption corrections by multi-scan were applied [28]. All non-hydrogen atoms were refined anisotropically. All bond lengths, angles, and isotropic parameters of the atoms found were checked thoroughly for any discrepancy. The model was then subjected to anisotropic refinement. The metal ion was first made anisotropic, then oxygen and nitrogen atoms followed by the carbons. All hydrogens were attached geometrically except for those bonded to hydroxyl oxygens which were located from a difference Fourier map. None of these hydrogens were refined, and they were made to ride on their respective atoms. Molecular structures of the complexes were drawn with the help of ORTEP and MERCURY [29, 30]. Measurement of hydrogen bonding was carried out by using PARST [31].

2.3. Preparation of complexes

2.3.1. Synthesis of [Cu(DNB)₂]. [Cu(DNB)₂] was prepared by 1 : 2 reaction of copper carbonate with 3,5-dinitrobenzoic acid in deionized water. The solution was stirred on a magnetic stirrer for 1 h at 60 °C. Crystals of [Cu(DNB)₂] were obtained on concentrating the reaction mixture. Decomposition of the powder product was found at 180–190 °C. Yield: 78%. IR (KBr) cm⁻¹: 3522 ($\nu(\text{OH})$, br), 3093 ($\nu(\text{=CH})$, s), 1630 ($\delta(\text{=CH})$, s), 1540 ($\nu(\text{NO}_2)_{\text{as}}$, s), 1318 ($\nu(\text{NO}_2)_{\text{s}}$, s), 1414 ($\delta(\text{=CH})_{\text{w}}$, br), 807 ($\delta(\text{-CH})$, s), 642 ($\delta(\text{=CH})$, s).

2.3.2. Synthesis of [Cu(THEEN)(DNB)] (DNB) (1). Complex **1** was synthesized by dissolving [Cu(DNB)₂] (0.487 g, 0.001 mol) and THEEN (0.0236 g, 0.001 mol) in an ethanol–water mixture. The mixture was stirred on a magnetic stirrer, put on a water bath for evaporation, and then left at room temperature. Change in light blue color of the [Cu(DNB)₂] solution to dark blue during addition of the ligand indicates that reaction is complete. The small blue crystals were obtained after a few days. The melting point of the crystals was 165 °C. Yield: 80%. IR (KBr) cm⁻¹: 3432 ($\nu(\text{-OH})$, br), 3092 ($\nu(\text{C-H})$, br), 2911 ($\nu(\text{C-H})$, br), 1624 ($\delta(\text{=CH})$, s), 1542 ($\nu(\text{NO}_2)_{\text{as}}$, s), 1454 ($\nu(\text{C-H})$), 1346 ($\nu(\text{NO}_2)_{\text{s}}$, s), 1189 ($\delta(\text{C-O})$, s), 911 ($\delta(\text{C-H})$), 798 ($\delta(\text{=CH})$, s), 724 ($\delta(\text{=CH})$). Elemental Analysis: Anal. Calcd for C₂₄H₃₀CuN₆O₁₆: C, 39.13; H, 4.49; N, 11.20. Found: C, 39.88; H, 4.15; N, 12.46%.

2.3.3. Synthesis of [Cu(TEAH₃)₂] (DNB)₂ (2). Complex **2** was synthesized by dissolving [Cu(DNB)₂] (0.487 g, 0.001 mol) and TEAH₃ (0.149 g, 0.001 mol) in an ethanol–water mixture. The mixture was stirred for 2 h with heating at 40–50 °C and then left to cool at room temperature. Change in light sky-blue color of the solution during the addition of TEAH₃ indicated completion of reaction. Dark blue crystals were obtained after evaporation at room temperature. Recrystallization was done by slow evaporation in ethanol–water mixture, and small crystals were obtained after 3–4 days. The melting point of the crystals was 145 °C. IR (KBr) cm⁻¹: 3353 ($\nu(\text{OH})$, br), 3092 ($\nu(\text{C-H})$, br), 2931 ($\nu(\text{C-H})$, br), 1623 ($\delta(\text{=CH})$, str), 1545 ($\nu(\text{NO}_2)_{\text{as}}$, s), 1427 ($\nu(\text{C-H})$), 1346 ($\nu(\text{NO}_2)_{\text{s}}$, s), 1140 ($\nu(\text{C-O})$, s), 925 ($\delta(\text{C-H})$), 797 ($\delta(\text{=CH})$, s), 721 ($\delta(\text{=C-H})$, s). Elemental Analysis: Anal. Calcd for C₂₆H₃₆CuN₆O₁₈: C, 38.97; H, 4.11; N, 11.03. Found: C, 39.79; H, 4.59; N, 11.47%.

2.4. Antimicrobial evaluation

Antimicrobial screening of the synthesized metal complexes and the metal salt for their biological activity was carried out using the microbroth dilution method [32]. The complexes were tested against pathogenic Gram(–) bacteria (*S. marcescens*, *S. japonicum*, *S. maltophilia*), Gram(+) bacteria (*S. aureus*), and fungal species (*Candida albicans*, *Aspergillus niger*, and *Saccharomyces cerevisiae*). The minimum inhibitory concentration (MIC) was taken as the lowest concentration of metal complex or tested antibacterial agent that shows no visible bacterial growth. Serial dilutions of the test complexes and reference drug were prepared. Test compounds were dissolved in DMSO, and further progressive dilutions were made to obtain required concentration. To ensure that the solvent had no effect on the bacterial growth, a control was performed with the test medium supplemented with DMSO at the same dilutions as used in the experiments; DMSO had no effect on the microorganisms in the concentrations studied.

2.5. Cell culture, growth conditions, and treatments

Human breast cancer MCF-7 cell line, human leukemia HL-60 cell line, and human colon cancer HCT-116 cell line were obtained from European Collection of Cell Cultures (ECACC). The cell lines were grown in minimum essential (MEM) and RPMI-1640 medium supplemented with 10% heat inactivated FBS, penicillin (100 units/mL), streptomycin (100 µg/mL), L-glutamine (0.3 mg/mL), and NaHCO₃ (3.8 mg/mL). Cells were grown in a CO₂ incubator (Thermocon Electron Corporation, USA) at 37 °C in a 5% CO₂ humidified atmosphere for 24 h. Adherent cells grown in monolayer cultures were detached with trypsin (0.1% w/v)/EDTA (1 mM) solution. Soon after cells were ready to detach, the trypsin/EDTA solution was removed. Cells were dispersed gently by pipetting in complete growth medium, centrifuged at 200 × g, 4 °C for 5 min. Required cell suspensions (0.6 × 10⁴/100 µL) were distributed into a 96-well plate and incubated in a CO₂ incubator. After 16 h, cells were refreshed with fresh complete medium. Cells grown in semi-confluent stage (approx. 70% confluent) were treated with tested material while the untreated control cultures received only DMSO (<1%).

2.6. Computational details

The quantum chemical calculations (DFT calculations) giving molecular geometries of minimum energies, molecular orbitals (HOMO-LUMO), and vibrational spectra were performed using the Gaussian 03 (Revision B.04) package [33]. Molecular orbitals are visualized using “Gauss view.” The method used was Becke’s three-parameter hybrid-exchange functional, the nonlocal correlation provided by Lee, Yang, and Parr expression, and the Vosko, Wilk, and Nair 1980 local correlation functional (III) (B3LYP) using DMSO as solvent [34]. The 6-31G basis set was used for C, N, and O. The LANL2DZ basis set [35] and pseudopotentials of Hay and Wadt were used for Cu [36]. The input coordinates are obtained from the crystal structure data. Only the primary coordination sphere of copper in **1** and **2** has been optimized. The structural parameters were adjusted until an optimal agreement between calculated and experimental structure was obtained throughout the entire range of available structures.

3. Results and discussion

3.1. Description of crystal structures

The X-ray crystal structure of **1** reveals that the molecular structure consists of one Cu(II), two dinitrobenzoate anions, and one THEEN as shown in figure 1(a). The crystal data and refinement details of both complexes are given in table 1.

Selected bond distances, bond angles, and hydrogen bonding geometry are listed in tables 2 and 3, respectively. The crystal structure shows that [Cu(THEEN)(DNB)](DNB) is a

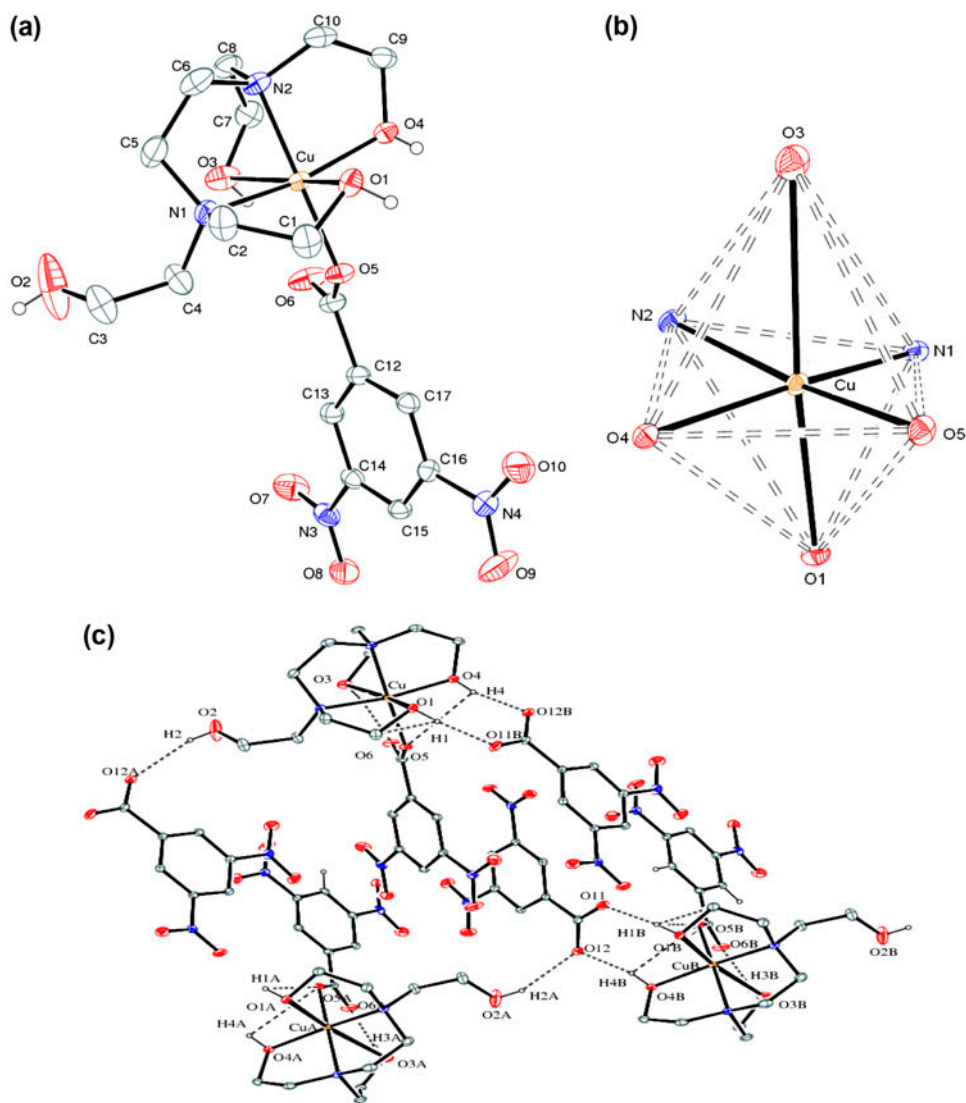


Figure 1. (a) ORTEP diagram of **1** with atom labeling scheme. Hydrogens attached to carbon have been removed for clarity. (b) Distorted octahedral view around Cu(II). (c) Molecular structure of **1** with hydrogen-bonding interactions.

Table 1. Crystallographic data and structure refinement parameters for **1** and **2**.

	1	2
Empirical formula	C ₂₄ H ₃₀ CuN ₆ O ₁₆	C ₂₆ H ₃₆ CuN ₆ O ₁₈
Formula weight	722.09	784.16
Crystal system	Monoclinic	Monoclinic
Crystal size	0.14 × 0.12 × 0.10	0.14 × 0.12 × 0.09
Color	Blue	Blue
Shape	Needle	Rectangular
Space group	<i>P</i> -2 ₁	<i>P</i> 2 ₁ / <i>c</i>
Unit cell dimensions		
<i>a</i> (Å)	11.321(3)	15.2230(6)
<i>b</i> (Å)	9.923(2)	8.4710(4)
<i>c</i> (Å)	13.508(3)	13.2550(7)
α (°)	90	99.00
β (°)	99.735(10)	114.52(2)
γ (°)	90	90.00
Volume (Å ³)	1495.81(6)	1555.05(13)
<i>Z</i>	2	2
ρ_{Calcd} (g cm ⁻³)	1.603	1.675
μ (cm ⁻¹)	0.817	0.798
<i>F</i> _(0 0 0)	746	814
θ Range of data collection	1.53–31.65°	1.47–29.69°
Limiting frequency	–16 ≤ <i>h</i> ≤ 16	–21 ≤ <i>h</i> ≤ 20
	–8 ≤ <i>k</i> ≤ 14	–10 ≤ <i>k</i> ≤ 11
	–19 ≤ <i>l</i> ≤ 19	–15 ≤ <i>l</i> ≤ 18
Total reflections	19,979	16,412
Independent reflections	7469 [<i>R</i> (int) = 0.0206]	4356 [<i>R</i> (int) = 0.0237]
Completeness to $\theta = 25.00$	99.8%	98.9%
Data/restraints/parameters	7469/5/436	4356/3/241
Refinement method	Full matrix least squares on <i>F</i> ²	Full matrix least squares on <i>F</i> ²
Goodness of fit on <i>F</i> ²	1.030	1.045
Final <i>R</i> indices [<i>I</i> > 2 (<i>I</i>)]	<i>R</i> 1 = 0.0286, <i>wR</i> 2 = 0.0740	<i>R</i> 1 = 0.0273, <i>wR</i> 2 = 0.0763
<i>R</i> indices (all data)	<i>R</i> 1 = 0.0348, <i>wR</i> 2 = 0.0772	<i>R</i> 1 = 0.0327, <i>wR</i> 2 = 0.0792
Largest diff. peak and hole (e Å ⁻³)	0.365 and –0.317	0.397 and –0.373
CCDC	919,842	933,764

Table 2. Selected bond distances (Å) and angles (°) for **1** and **2**.

Bond lengths	Experimental	Calculated	Dev.	Bond angles	Experimental	Calculated	Dev.
Complex 1							
Cu–N1	2.085	2.291	–0.206	N1–Cu–N2	87.84	86.00	1.84
Cu–N2	2.030	2.073	–0.043	N1–Cu–O1	80.14	77.60	2.54
Cu–O1	2.336	2.163	0.173	N1–Cu–O3	89.26	104.00	–14.74
Cu–O3	2.653	2.035	0.618	N1–Cu–O4	165.82	153.10	12.72
Cu–O4	2.015	2.322	–0.307	N1–Cu–O5	97.42	100.60	–3.17
Cu–O5	1.961	1.970	–0.008	O1–Cu–O4	90.97	82.40	8.56
				O1–Cu–O5	88.91	86.50	2.41
Complex 2							
Cu–N1	2.071	2.118	–0.046	N1–Cu–O1	85.35	84.40	0.95
Cu–O1	2.021	2.044	–0.023	N1–Cu–O2	101.34	78.70	22.64
Cu–O2	2.298	2.353	–0.055	O1–Cu–O2	92.12	87.92	4.20

mononuclear complex with distorted octahedral Cu(II) [figure 1(b)]. THEEN is a pentadentate ligand coordinating to Cu(II) through both its amine nitrogens N1, N2, and three terminal hydroxyl oxygens O1, O3, and O4. One dinitrobenzoate is bound directly

Table 3. Selected hydrogen bond interactions (\AA , $^\circ$) for **1** and **2**.

D–H \cdots A	d(D–H)	d(H–A)	d(D–A)	$\angle(\text{DHA})$
Complex 1				
O1–H1 \cdots O5	0.84	2.902	3.003	92
O1–H1 \cdots O11B	0.84	1.858	2.652	176
O2–H2 \cdots O12A	0.85	2.254	3.004	159
O3–H3 \cdots O6	0.85	1.893	2.638	152
O4–H4 \cdots O12B	0.80	1.795	2.544	168
Complex 2				
O1–H1 \cdots O5A	0.82	1.749	2.538	181
O2–H2 \cdots O3B	0.82	1.884	2.672	174
O3–H3 \cdots O4C	0.80	1.876	2.639	170

through the carboxylate oxygen. The second dinitrobenzoate anion is outside the coordination sphere interacting indirectly with copper through hydrogen bonds. A partially charge-separated complex is formed. Complex **1** shows both intermolecular and intramolecular hydrogen-bonding interactions involving the oxygens belonging to hydroxyl, carboxylate, and the nitro-groups of the benzoate anions [figure 1(c)]. The polar hydroxyl groups of the ligand act as H-bond donors toward the benzoate oxygen acceptors (table 3). The center-to-center distance between the two phenyl rings of 4.059 \AA indicates face-to-face π – π interaction between two phenyl rings.

In the crystal structure of $[\text{Cu}(\text{TEAH}_3)_2](\text{DNB})_2$, two triethanolamine (TEAH_3) are tridentate, coordinating to Cu(II) through four oxygens and two nitrogens [figure 2(a)], resulting in a distorted octahedron [figure 2(b)]. Both dinitrobenzoate anions are outside the coordination sphere giving a charge-separated complex. DNB^- and $[\text{Cu}(\text{TEAH}_3)_2]^{2+}$ interact indirectly with each other through hydrogen-bonding interactions.

The hydrogen bonds are between coordinated hydroxyl oxygens of TEAH_3 and oxygen of the dinitrobenzoate. O5 belonging to carboxylate of DNB^- is an acceptor of hydrogen bonds from terminal hydroxyl oxygen of the neighboring molecular units. The terminal hydroxyl oxygens are donors of hydrogen bonds and also acceptors from the other molecules in the unit cell [figure 2(c), table 3].

Both **1** and **2** exhibit Jahn–Teller effects, apparent from the relatively longer distances of the axial oxygens Cu–O1, Cu–O3 in **1** and Cu–O2, Cu–O2' in **2** (table 2). The mode of coordination of THEEN and TEAH_3 with Cu(II) varies under the influence of different counter-anions resulting in different geometries by the resultant complexes. For instance, with Cu(II) and THEEN, with perchlorate, a dinuclear complex is formed [37]. With picrate as counter-anion, a mononuclear complex is formed with square pyramidal geometry [25]a. Similarly, with picrate, TEAH_3 coordinates tetradentate to Cu(II) leading to a partially charge-separated mononuclear complex with square pyramidal geometry [25(a)]. Similarly, dimeric, trimeric, tetrameric, and polymeric structures of triethanolamine with Cu(II) with different anions have been reported [24].

3.2. Electronic spectra

Absorption spectra of the Cu(II) complexes were recorded in DMSO at room temperature (figure 3). Complexes **1** and **2** displayed intense high energy bands at 299 nm ($33,449$ – $34,246 \text{ cm}^{-1}$, $\epsilon = 910 \text{ M}^{-1} \text{ cm}^{-1}$) and 310 nm ($32,258$ – $37,037 \text{ cm}^{-1}$, $\epsilon = 980 \text{ M}^{-1} \text{ cm}^{-1}$), attributed to ligand-to-metal charge-transfer transitions [38]. The electronic spectra displayed a broad d–d band at 724 nm ($13,812 \text{ cm}^{-1}$, $\epsilon = 59 \text{ M}^{-1} \text{ cm}^{-1}$) and at 768 nm

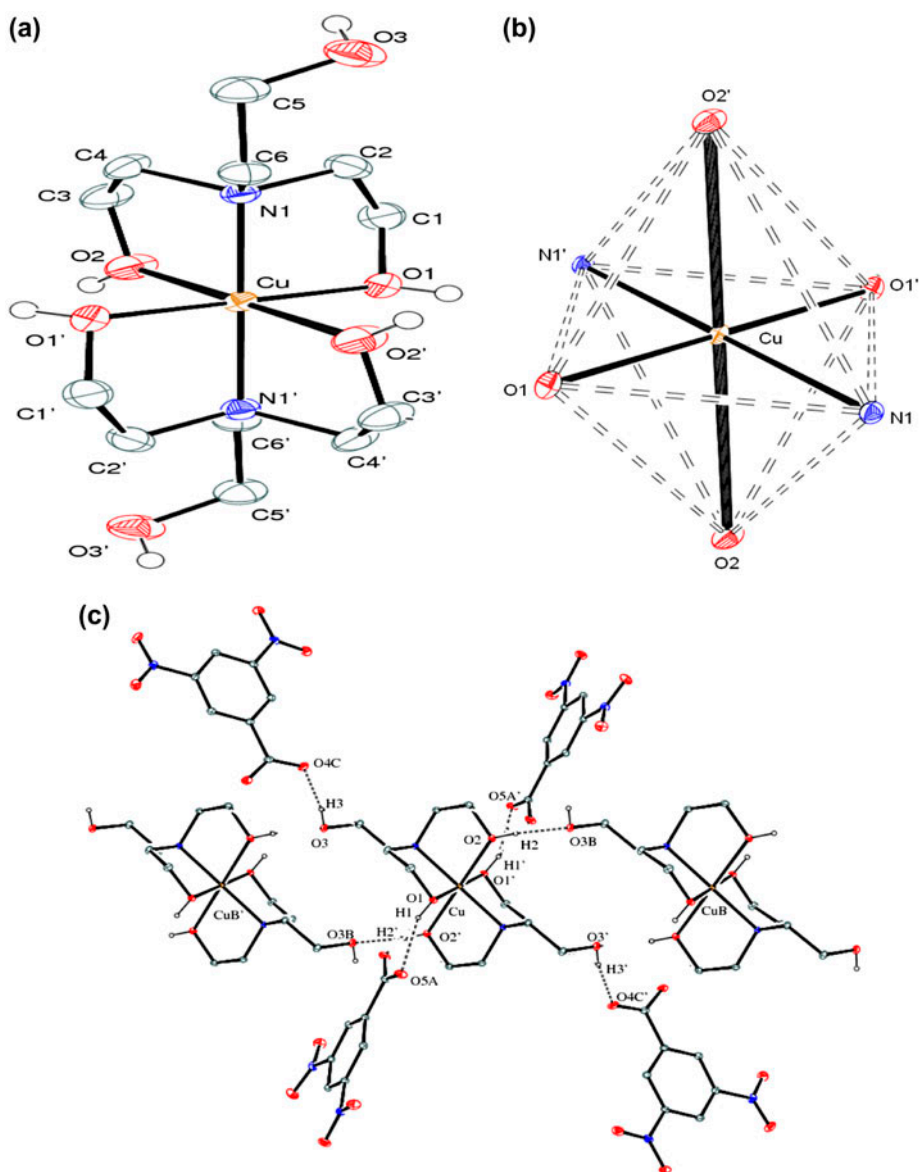


Figure 2. (a) ORTEP diagram of **2** with atom labeling scheme. The anions and the hydrogens attached to the carbon have been removed for clarity. (b) Distorted octahedral view around Cu(II). (c) Molecular structure of the complex with hydrogen-bonding interactions.

(13,020–13,072 cm^{-1} , $\epsilon = 91 \text{ M}^{-1} \text{ cm}^{-1}$) for **1** and **2**, respectively, indicating a distorted octahedral geometry. Broadness may be attributed to Jahn–Teller distortions [39]. These bands are assigned to overlapping transitions, d_{xz} , $d_{yz} \rightarrow d_{x^2-y^2}$, $d_{xy} \rightarrow d_{x^2-y^2}$, $d_z^2 \rightarrow d_{x^2-y^2}$. The electronic spectra of these complexes were calculated with the DFT method displaying a broad absorption in the UV–vis region consistent with the experimental spectra (figure S3).

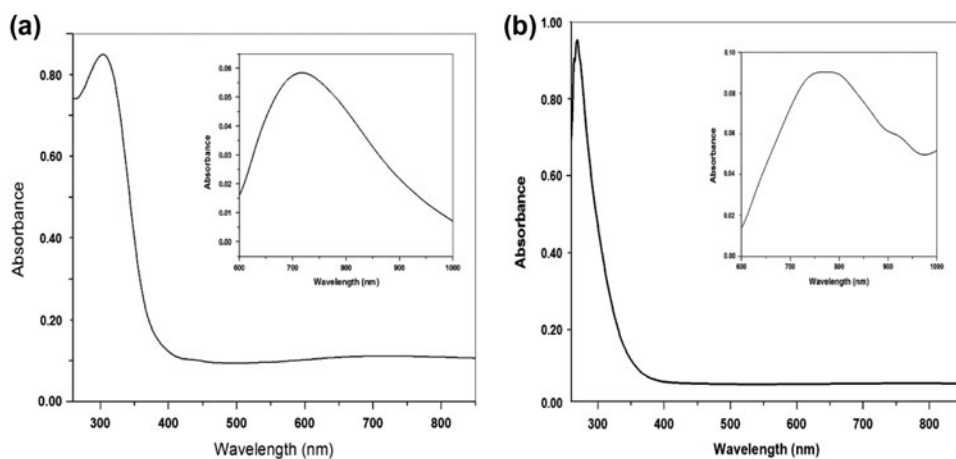


Figure 3. UV-vis spectrum of (a) [Cu(THEEN)(DNB)](DNB) (**1**) and (b) [Cu(TEAH₃)₂](DNB)₂ (**2**) in DMSO.

3.3. EPR spectral studies

EPR spectra of **1** and **2** were recorded as polycrystalline samples at room temperature, with X-band frequency of 9.1 GHz under magnetic field strength of 3000 G (figure 4). The spectral values revealed a well-resolved signal with $g_{\parallel} = 2.26$ and $g_{\perp} = 2.06$ for **1** and $g_{\parallel} = 2.21$ and $g_{\perp} = 2.05$ for **2**, indicating that the unpaired electron is localized in the $d_{x^2-y^2}$ orbital of Cu(II), consistent with a distorted octahedron elongated along the z axis [40, 41]. Further g_{\parallel} and g_{\perp} values were related to each other by the expression $G = (g_{\parallel} - 2)/(g_{\perp} - 2)$, and it predicted the exchange interactions in the complexes. If $G > 4$, then the local tetragonal axis are aligned parallel or only slightly misaligned, and if $G < 4$, significant exchange coupling is present. The observed values for the exchange interaction parameter ($G = 4.3$ and 4.2) indicate that the local tetragonal axis is aligned parallel or slightly misaligned and the unpaired electron is present in the $d_{x^2-y^2}$ orbital. For **1** and **2**, g_{\parallel} is a moderately sensitive

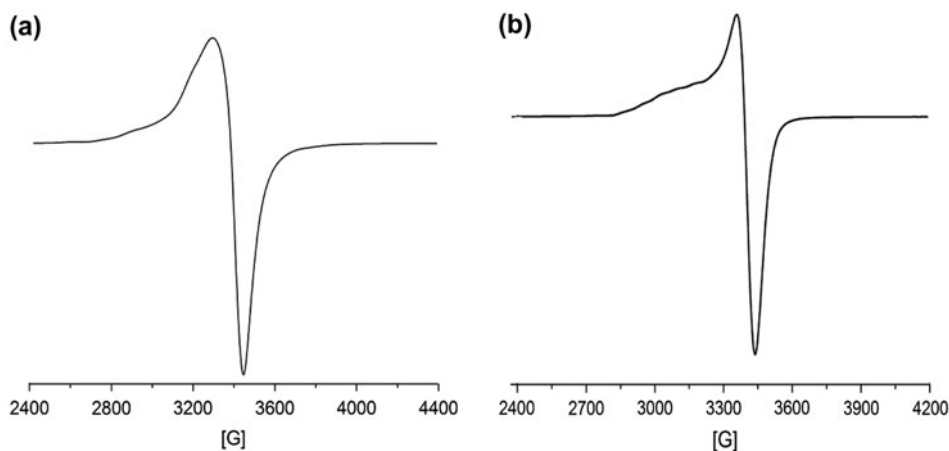


Figure 4. EPR spectrum of polycrystalline samples of (a) [Cu(THEEN)(DNB)](DNB) (**1**) and (b) [Cu(TEAH₃)₂](DNB)₂ (**2**).

parameter to indicate covalence. In case of covalent environment $g_{||} < 2.3$ and for ionic environment $g_{||} \geq 2.3$. The g values obtained for this complex were less than 2.3, in agreement with the covalent character of metal ligand bond [42].

3.4. Computational discussion

We correlate the structural parameters obtained from crystal structure studies with computational data. The structural parameters have been calculated, vibrational modes assigned, and HOMO-LUMO energy gaps evaluated by performing DFT method with DMSO as solvent. Figure 5 shows the optimized molecular structure and coordination sphere for **1** and **2**. Only the primary coordination spheres of the metal ion are optimized here. Selected bond lengths and angles are given in table 2 as space restrictions do not allow the complete listing of calculated bond lengths, bond angles for both complexes. Both geometric structures were identified, and after optimization are close to the experimental structures. The optimized geometry analysis reveals that the observed and calculated positions of the metal and donors are in agreement. The energy minimized structures reproduced the observed X-ray structures with a maximum deviation of 0.61 and 0.055 Å for **1** and **2**, respectively, in the Cu–L bond lengths.

The maximum deviation in L–M–L bond angles is 14.74° and 22.64° in **1** and **2**, respectively (table 2, figures S1 and S2 [see online supplemental material at <http://dx.doi.org/10.1080/00958972.2015.1031120>]). The small discrepancies in bond lengths and bond angles are attributable to H-bonding and packing interactions within the lattice which are not modeled during computational study.

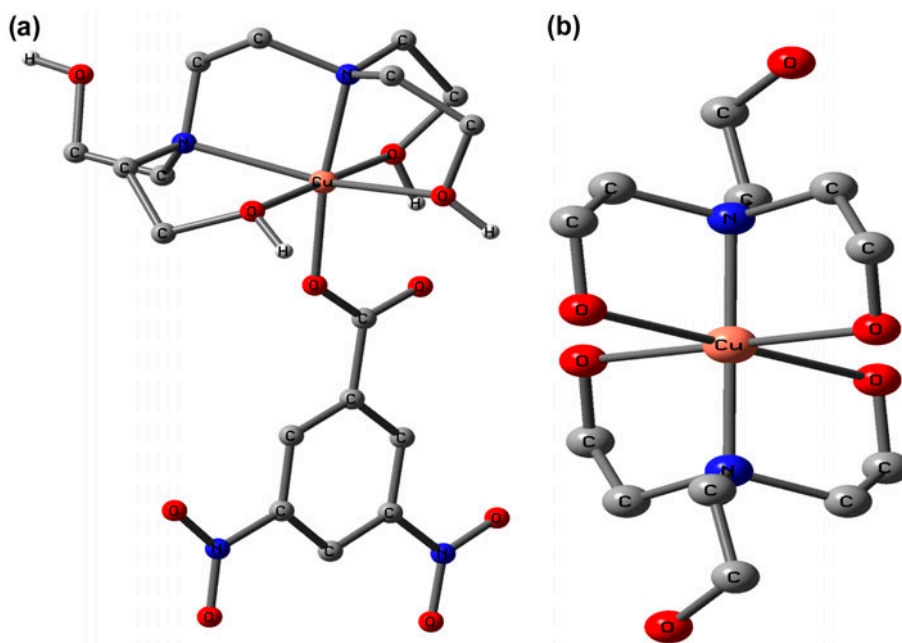


Figure 5. Optimized geometries of (a) $[\text{Cu}(\text{THEEN})(\text{DNB})]^+$ (**1**) and (b) $[\text{Cu}(\text{TEAH}_3)_2]^{2+}$ (**2**). DNB^- are excluded for clarity.

The frontier molecular orbital energies have been calculated with B3LYP/6-31G/LANL2DZ level of theory using DMSO as solvent. The highest occupied molecular orbital (HOMO) is distributed over the coordinated as well as non-coordinated hydroxyl oxygen and on copper in **1**, whereas LUMO is mainly concentrated over nitro-group of the dinitrobenzoate. In **2**, the HOMO is concentrated over the non-coordinated hydroxyl oxygen as well as on the amine nitrogen of TEAH₃ and LUMO is mainly distributed over the coordinated hydroxyl oxygens, amine nitrogens and also on copper (figure 6). The HOMO-LUMO energy gap (HLG) values are 3.075 and 3.592 eV for **1** and **2**, respectively. HLG is a critical parameter in determining electrical transport properties because it is a measure of electron conductivity. Moreover, HOMO and LUMO energy gap suggests charge-transfer interactions taking place within the molecules [43].

Vibrational spectroscopy has been used as a standard tool for characterization of molecular systems by DFT calculations with calculated frequencies by Gaussian 03 closer to the experimental values. Experimental and calculated vibration frequencies along with corresponding vibrational assignments are given in table 4. A small discrepancy found in the absorption band assigned to hydroxyl group is attributable to H-bonding interactions which are not modeled in the optimized structures.

3.5. Antimicrobial activity

The MIC values for **1** and **2**, defined as the lowest concentration of the compound preventing visible growth, were determined using microbroth dilution method. The results are

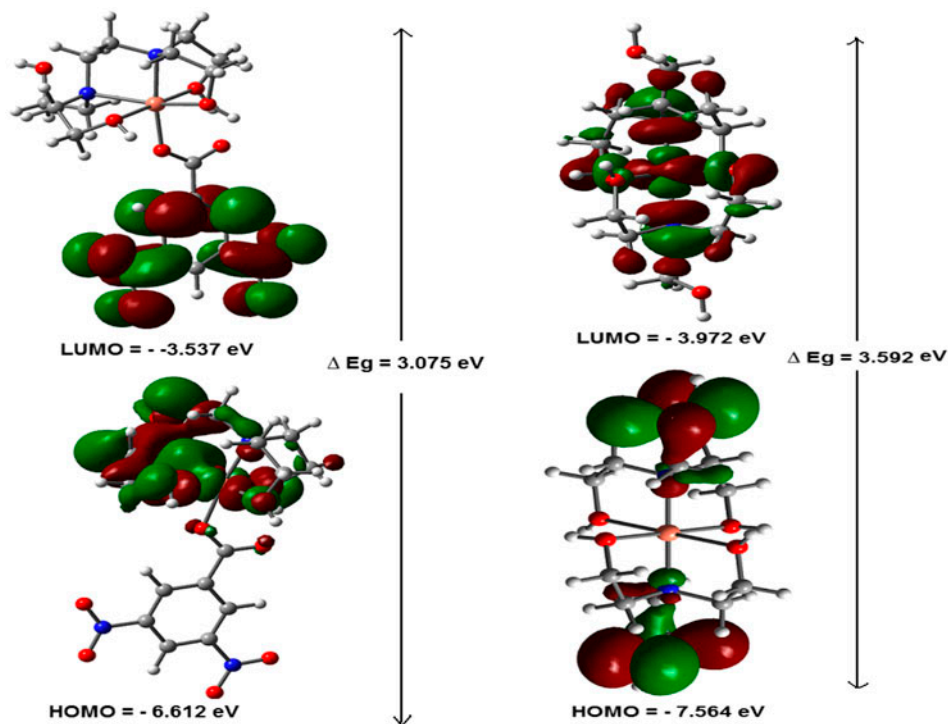


Figure 6. Frontier molecular orbital surfaces (HOMO-LUMO) for **1** and **2** with their energy gaps.

Table 4. Selected experimental IR and calculated vibrational frequencies (cm^{-1}) for **1** and **2**.

Assignment	Complex 1		Complex 2	
	Experimental	Theoretical	Experimental	Theoretical
$\nu(\text{OH})$	3432 br	3289, 3680	3353 vs	3667, 3198
$\nu(\text{C-H})$	2911 br	3018	2931s	3039
$\delta(=\text{CH})$	1624 vs	1647	1623 vs	1566
$\nu(\text{NO}_2)_{\text{as}}$	1542 s	1557	1545 s	1546
$\nu(\text{NO}_2)_{\text{s}}$	1346 vs	1333	1346 vs	1364
$\delta(\text{C-O})_{\text{str}}$	1189 s	1190	1140 s	1136
$\delta(=\text{CH})$	724 m	722	721 m	739

depicted in table 5. Complex **1** is an excellent antimicrobial agent against *S. aureus* and *S. marcescens*, whereas no inhibition activity was found against *S. maltophilia* and *S. japonicum* [figure 7(a)]. The results obtained in the present work are in contrast to the results reported earlier for $[\text{Cu}(\text{THEEN})(\text{H}_2\text{O})](\text{PIC})_2$ against all bacterial strains except against *S. marcescens* [25]. Similarly, **2** and the previously reported complex $[\text{Cu}(\text{TEAH}_3)(\text{PIC})](\text{PIC})\cdot\text{H}_2\text{O}$ have exhibited different behavior against the above selected bacterial strains except against *S. maltophilia*. From this discussion, it can be concluded that there is a large influence of the counter-anion on the action of complexes against bacterial strains. Also the chelation of ligands with metal ion increases the biological activity as reported earlier [25].

Table 5. MICs for the complexes and the metal salt ($\mu\text{g}/\text{mL}$) on bacterial strains by microbroth dilution method.

Compounds	<i>Staphylococcus aureus</i>	<i>Serratia marcescens</i>	<i>Stenotrophomonas maltophilia</i>	<i>Sphingobium japonicum</i>
THEEN	25	25	50	25
TEAH ₃	50	50	25	50
DNB	50	25	12.5	50
$[\text{Cu}(\text{DNB})_2]$	25	25	3.2	25
1	3.2	6.2	x	x
2	12.5	50	1.5	3.2
Ciprofloxacin	3.2	3.2	6.2	1.5

x = no inhibition.

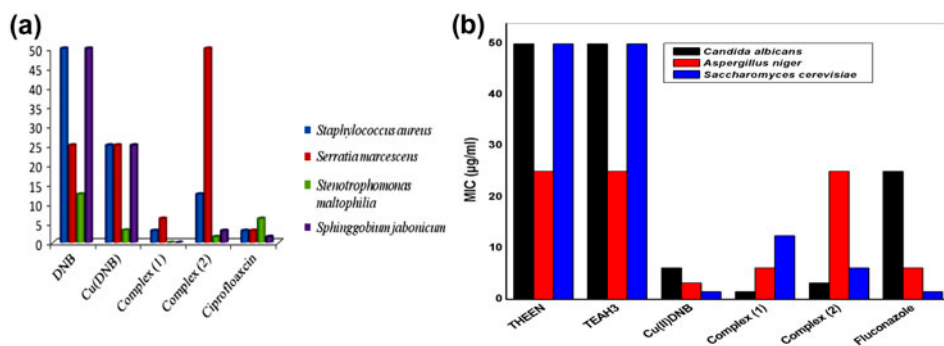


Figure 7. (a) Antimicrobial activity of complexes with MIC in ($\mu\text{g}/\text{mL}$). (b) Antifungal activity of complexes with MIC in ($\mu\text{g}/\text{mL}$).

Table 6. MICs for the complexes and the metal salt ($\mu\text{g/mL}$).

Compounds	<i>Candida albicans</i>	<i>Aspergillus niger</i>	<i>Saccharomyces cerevisiae</i>
THEEN	50	25	50
THPEN	25	50	25
TEAH ₃	50	25	50
Cu(II) DNB	6.2	3.2	1.5
1	1.5	6.2	12.5
2	3.2	25	6.2
Fluconazole	25	6.2	1.5

A comparative study of the metal salt and its complexes indicates that complexes exhibit higher antimicrobial activity than the metal salts. This proves that chelation of ligands with metal ions increases the biological activity as reported [44]. This may be due to increased lipophilicity which enhances the penetration of complexes into the lipid membranes blocking the metal binding sites in the enzymes of microorganisms; they also disturb the respiration process of the cell, and thus, the synthesis of the proteins that restricts further growth of organisms [39, 45].

The ligands, copper dinitrobenzoate, **1** and **2** are also effective antifungal agents when tested on fungi *C. albicans*, *A. niger*, and *S. cerevisiae* [table 6, figure 7(b)]. Copper(II) dinitrobenzoate and its complexes are better antifungal agents than the ligands. **1** and **2** are more effective against *C. albicans* than *A. niger* and *S. cerevisiae* with relatively lower MIC than Fluconazole.

3.6. Cell proliferation assay (MTT)

The *in vitro* cytotoxicities of the complexes have been evaluated against 3-cell line panel consisting of human breast cancer MCF-7, human leukemia HL-60, and human colon cancer HCT-116, respectively. MTT assay is a quantitative colorimetric method for the determination of cell survival and proliferation. The assessed parameter is the metabolic activity of viable cells. Metabolically active cells reduce pale yellow tetrazolium salt (MTT) to a dark blue water-insoluble formazan, which can be quantified after solubilization with DMSO. The absorbance of the formazan correlates directly to the number of viable cells. Cells were seeded in 96-well plates at a density of 6000 cell/well in 100 μL of medium per well overnight. Next day, cultures were incubated with different concentrations of **1** and **2** and incubated for 48 h. The dye at a concentration of 2.5 mg/mL MTT was added for 4 h.

Table 7. IC₅₀ values of cell viability assay for MCF-7, HCT-116 and HL-60 cells.

Complex	Conc. ($\mu\text{g/mL}$)	MCF-7		HCT-116		HL-60	
		Growth inhibition (%)	IC ₅₀ ($\mu\text{g/mL}$)	Growth inhibition (%)	IC ₅₀ ($\mu\text{g/mL}$)	Growth inhibition (%)	IC ₅₀ ($\mu\text{g/mL}$)
1	10	30	86	11	>100	30	46
	30	42		25		38	
	100	59		38		87	
2	10	47	23	18	>100	21	37
	30	59		23		42	
	100	70		33		93	

The supernatant was aspirated and MTT-formazan crystals dissolved in 150 μL DMSO; OD was measured at $\lambda = 540$ nm (reference wavelength, $\lambda = 620$ nm) on an ELISA reader (BioTek). Cell growth was calculated by comparing the absorbance of treated *versus* untreated cells [46]. Complex **2** was most active in MCF-7 cell lines with IC_{50} value of 23 $\mu\text{g}/\text{m}_1$ (table 7). Both **1** and **2** were inactive in colon cancer HCT-116 cells with IC_{50} value more than 100 $\mu\text{g}/\text{mL}$ [46]. The IC_{50} value of synthesized complexes compares well with those reported for cytotoxic copper(II) complexes giving IC_{50} values in similar concentration range [11–15]. This study suggests that **1** and **2** have potential as anticancer agents.

4. Conclusion

[Cu(THEEN)(DNB)](DNB) (**1**) and [Cu(TEAH₃)₂](DNB)₂ (**2**) have been synthesized and structurally characterized. Extensive hydrogen-bonding interactions are present in **1** and **2**. The counter-anion influences the nature and acquired geometry of the complexes and also their biological activity. [Cu(THEEN)(DNB)](DNB) (**1**) is partially charge-separated, whereas [Cu(THEEN)(H₂O)](PIC)₂ formed a charge-separated complex. Similarly, [Cu(TEAH₃)₂](DNB)₂ (**2**) forms a charge-separated complex in the present study, whereas [Cu(TEAH₃)(PIC)](PIC)·H₂O formed a partially charge-separated complex in previous work. **1** and **2** have distorted octahedral geometry and underwent Jahn–Teller distortion. Previously reported complexes of copper picrate with THEEN and TEAH₃ had square pyramidal geometry with coordination number five. **1** and **2** are more selective antimicrobial agents against some bacterial strains than similar reported complexes of copper and silver picrate. The complexes exhibit *in vitro* cytotoxicity toward MCF-7, HCT-116, and HL-60 cells. The IC_{50} values of the complexes have been determined by the MTT assay.

The theoretical and experimental parameters of optimized structures are in agreement. The accuracy of results predict that the DFT studies performed at B3LYP/LANL2DZ level is the appropriate quantum chemical method for reproducing the experimental results for **1** and **2**. The small discrepancies in geometric parameters are attributable to H-bonding and packing interactions within the lattice which are not modeled during computational study. The calculated HOMO-LUMO energy gaps suggest that charge-transfer transitions take place within the complexes.

Acknowledgements

We are highly thankful to Ministry of Human Resource and Development (MHRD), New Delhi for providing research assistantship to Mr Rakesh Kumar, one of the authors, and Dr B. R. Ambedkar National Institute of Technology, Jalandhar for providing research infrastructure. Rakesh Kumar is also thankful to Ms Isha for their valuable help to carrying out the UV-vis spectral studies.

Disclosure statement

No potential conflict of interest was reported by the authors.

Supplementary data

CCDC 919842 and 933764 contain the supplementary crystallographic data for the present complexes. This data can be obtained free of charge via <http://www.ccdc.cam.ac.uk/conts/retrieving.html>, or from the Cambridge Crystallographic Data Center, 12 Union Road, Cambridge CB2 1EZ, UK; Fax: (+44) 1223 336 033; or E-mail: deposit@ccdc.cam.ac.uk.

References

- [1] B.J. Hathway. In *Comprehensive Coordination Chemistry*, G. Wilkinson, R.D. Gillard, J.A. McCleverty (Eds.), Vol 5, pp. 533–594, Pergamon Press, Oxford (1987).
- [2] S. Mandal, G. Das, R. Singh, R. Shukla, P.K. Bharadwaj. *Coord. Chem. Rev.*, **160**, 191 (1997).
- [3] D.R. McMillin. *J. Chem. Educ.*, **62**, 997 (1985).
- [4] E. Bouwman, W.L. Driessen, J. Reedijk. *Coord. Chem. Rev.*, **104**, 143 (1990).
- [5] (a) M. Frezza, S. Hindo, D. Chen, A. Davenport, S. Schmitt, D. Tomco, Q.P. Dou. *Curr. Pharm. Des.*, **16**, 1813 (2010); (b) S.J. Tan, Y.K. Yan, P.P. Lee, K.H. Lim. *Future Med. Chem.*, **2**, 1591 (2010); (c) B. Lippert. *Cisplatin: Chemistry and Biochemistry of a Leading Anticancer Drug*, Wiley-VCH, Weinheim (1999); (d) A.S.A. Surrah, M. Kettunen. *Curr. Med. Chem.*, **13**, 1337 (2006); (e) C.S. Allardyce, P.J. Dyson. *Platinum Met. Rev.*, **45**, 62 (2001); (f) K. Ghosh, P. Kumar, N. Tyagi, U.P. Singh, V. Aggarawal, M.C. Baratto. *Eur. J. Med. Chem.*, **45**, 3770 (2010); (g) C. Marzano, M. Pellei, F. Tisato, C. Santini. *Anticancer Agents Med. Chem.*, **9**, 185 (2009).
- [6] (a) P. Gamez, P.G. Aubel, W.L. Driessen. *J. Reedijk. Chem. Soc. Rev.*, **30**, 376 (2001); (b) K.D. Karlin, A.D. Zuberbuhler. In *Bioinorganic Catalysis*, J. Reedijk, E. Bouwman (Eds.), 2nd Edn, pp. 469–534. M. Dekker, New York (1999).
- [7] P. Uma Maheswari, F. Hartl, M. Quesada, F. Buda, M. Lutz, A.L. Spek, P. Gamez, J. Reedijk. *Inorg. Chim. Acta*, **374**, 406 (2011).
- [8] K.D. Karlin, Z. Tyeklar. *Bioinorganic Chemistry of Copper*, Chapman & Hall, New York (1993).
- [9] D. Karakas, K. Sayin. *Indian J. Chem.*, **52**, 480 (2013).
- [10] S. Itoh. In *Comprehensive Coordination Chemistry*, J.A. McCleverty, T.J. Meyer, L. Que, W.B. Tolman (Eds.), pp. 369–393, Elsevier, Dordrecht (2003).
- [11] C.-Z. Xie, M.-M. Sun, S.-H. Li, X.-T. Zhang, X. Qiao, Y. Ouyang, J.-Y. Xu. *J. Coord. Chem.*, **66**, 3891 (2013).
- [12] J. Zhao, K. Peng, Y. Guo, J. Zhang, D. Zhao, S. Chen, J. Hu. *J. Coord. Chem.*, **67**, 2344 (2014).
- [13] T.T. Xing, S.-H. Zhan, Y.-T. Li, Z.-Y. Wu, C.-W. Yan. *J. Coord. Chem.*, **66**, 3149 (2013).
- [14] S. Anbu, A. Killivalavan, E.C.B.A. Alegria, G. Mathan, M. Kandaswamy. *J. Coord. Chem.*, **66**, 3989 (2013).
- [15] W.A. Wani, Z. Al-Othman, I. Ali, K. Saleem, M.-F. Hsieh. *J. Coord. Chem.*, **67**, 2110 (2014).
- [16] K.G. Daniel, R.H. Harbach, W.C. Guida, Q.P. Dou. *Front. Biosci.*, **9**, 2652 (2004).
- [17] C. Marzano, M. Pellei, F. Tisato, C. Santini. *Anticancer Agents Med. Chem.*, **9**, 185 (2009).
- [18] B. Sarkar. *Chem. Rev.*, **99**, 2535 (1999).
- [19] N. Jiménez-Garrido, L. Perelló, R. Ortiz, G. Alzuet, M. González-Álvarez, E. Cantón, M. Liu-González, S. García-Granda, M. Pérez-Priede. *J. Inorg. Biochem.*, **99**, 677 (2005).
- [20] Z.H. Chohan, H.A. Shad, M.H. Youssoufi, T. Ben Hadda. *Eur. J. Med. Chem.*, **45**, 2893 (2010).
- [21] J.E. Weder, C.T. Dillon, T.W. Hambley, B.J. Kennedy, P.A. Lay, J.R. Biffin, H.L. Regtop, N.M. Davies. *Coord. Chem. Rev.*, **232**, 95 (2002).
- [22] (a) I. Iakovidis, I. Delimaris, S.M. Piperakis. *Mol. Biol Int.*, **2011**, 1 (2011); (b) R.P. Hertzberg, M.J. Caranfa, S.M. Hecht. *Biochemistry*, **28**, 4629 (1989); (c) M.B. Ferrari, F. Bisceglie, G. Pelosi, P. Tarasconi, R. Albertini, A. Bonati, P. Lunghi, S. Pinelli. *J. Inorg. Biochem.*, **83**, 169 (2001); (d) J.S. Lewis, J.M. Connett, J.R. Garbow, T.L. Buettner, Y. Fujibayashi, J.W. Fleshman, M.J. Welch. *Cancer Res.*, **62**, 445 (2002); (e) X.B. Yang, Q. Wang, Y. Huang, P.H. Fu, J.S. Zhang, R.Q. Zeng. *Inorg. Chem. Commun.*, **25**, 55 (2012).
- [23] (a) N. Komiya, T. Naota, Y. Oda, S.-I. Murahashi. *J. Mol. Catal. A: Chem.*, **117**, 21 (1997); (b) S. Murahashi, N. Komiya, Y. Hayashi, T. Kumano. *Pure Appl. Chem.*, **73**, 311 (2001).
- [24] A.M. Kirillov, M.N. Kopylovich, M.V. Kirillova, M. Haukka, M.F.C. da Silva, A.J.L. Pombeiro. *Angew. Chem. Int. Ed.*, **44**, 4345 (2005).
- [25] (a) R. Kumar, S. Obrai, A. Kaur, G. Hundal, H. Meehnian, A.K. Jana. *Polyhedron*, **56**, 55 (2013); (b) R. Kumar, S. Obrai, J. Mitra, A. Sharma. *Spectrochim Acta, Part A*, **115**, 244 (2013); (c) R. Kumar, S. Obrai, A. Kaur, M.S. Hundal, H. Meehnian, A.K. Jana. *New J. Chem.*, **38**, 1186 (2014).
- [26] A. Altomare, M.C. Burla, M. Camalli, G.L. Cascarano, C. Giacovazzo, A. Guagliardi, A.G.G. Moliterni, G. Polidori, R. Spagna. *J. Appl. Crystallogr.*, **32**, 115 (1999).
- [27] G.M. Sheldrick. *SHELXTL/PC Siemens, XCANS*, Siemens Analytical X-ray Instruments Inc., Madison, WI (1994).

- [28] G.M. Sheldrick. *SADABS Program for Empirical Absorption Correction*, University of Gottingen, Gottingen, Germany (1996).
- [29] L.J. Farrugia. *J. Appl. Crystallogr.*, **30**, 565 (1997).
- [30] F.H. Allen. *Acta Crystallogr., Sect. B Struct. Sci.*, **58**, 380 (2002).
- [31] M. Nardelli. *Comput. Chem.*, **7**, 95 (1983).
- [32] H.K. No, N.Y. Park, S.H. Lee, S.P. Meyers. *Int. J. Food Microbiol.*, **74**, 65 (2002).
- [33] M.J. Frisch, G.W. Trucks, H.B. Schlegel, G.E. Scuseria, M.A. Robb, J.R. Cheeseman, J.A. Montgomery, T. Vreven Jr., K.N. Kudin, J.C. Burant, J.M. Millam, S.S. Iyengar, J. Tomasi, V. Barone, B. Mennucci, M. Cossi, G. Scalmani, N. Rega, G.A. Petersson, H. Nakatsuji, M. Hada, M. Ehara, K. Toyota, R. Fukuda, J. Hasegawa, M. Ishida, T. Nakajima, Y. Honda, O. Kitao, H. Nakai, M. Klene, X. Li, J.E. Knox, H.P. Hratchian, J.B. Cross, C. Adamo, J. Jaramillo, R. Gomperts, R.E. Stratmann, O. Yazyev, A.J. Austin, R. Cammi, C. Pomelli, J.W. Ochterski, P.Y. Ayala, K. Morokuma, G.A. Voth, P. Salvador, J.J. Dannenberg, V.G. Zakrzewski, S. Dapprich, A.D. Daniels, M.C. Strain, O. Farkas, D.K. Malick, A.D. Rabuck, K. Raghavachari, J.B. Foresman, J.V. Ortiz, Q. Cui, A.G. Baboul, S. Clifford, J. Cioslowski, B.B. Stefanov, G. Liu, A. Liashenko, P. Piskorz, I. Komaromi, R.L. Martin, D.J. Fox, T. Keith, M.A. Al-Laham, C.Y. Peng, A. Nanayakkara, M. Challacombe, P.M.W. Gill, B. Johnson, W. Chen, M.W. Wong, C. Gonzalez, J.A. Pople, *Gaussian 03 (Revision B.04)*. Gaussian, Inc., Wallingford CT, (2004).
- [34] (a) A.D. Becke. *J. Chem. Phys.*, **98**, 5648 (1993); (b) C. Lee, W. Yang, R.G. Parr. *Phys. Rev. B*, **37**, 785 (1988).
- [35] G.A. Petersson, M.A. Al-Laham. *J. Chem. Phys.*, **94**, 6081 (1991).
- [36] (a) P.J. Hay, W.R. Wadt. *J. Chem. Phys.*, **82**, 270 (1985); (b) W.R. Wadt, P.J. Hay. *J. Chem. Phys.*, **82**, 284 (1985).
- [37] A.S. de Sousa, M.A. Fernandes. *Polyhedron*, **21**, 1883 (2002).
- [38] A.A. Kamnev, A.G. Shchelochkov, Y.D. Perfiliev, P.A. Tarantilis, M.G. Polissiou. *J. Mol. Struct.*, **563–564**, 565 (2001).
- [39] (a) S. Tabassum, M. Zaki, F. Arjmand, I. Ahmad. *J. Photochem. Photobiol., B*, **114**, 108 (2012); (b) I. Lumb, M.S. Hundal, M. Corbella, V. Gomez, G. Hundal. *Eur. J. Inorg. Chem.*, **27**, 4799 (2013); (c) I. Lumb, M.S. Hundal, G. Hundal. *Inorg. Chem.*, **53**, 7770 (2014).
- [40] A.W. Addison. Copper coordination chemistry. In *Biochemical and Inorganic Perspectives*, K.D. Karlin, J. Zubieta (Eds.), p. 109, Adenine, Guilderland, NY (1983).
- [41] S. Tabassum, R.A. Khan, F. Arjmand, A.S. Juvekar, S.M. Zingde. *Eur. J. Med. Chem.*, **45**, 4797 (2010).
- [42] D. Kivelson, R. Neiman. *J. Chem. Phys.*, **35**, 149 (1961).
- [43] K. Fukui. *Science*, **218**, 747 (1982).
- [44] (a) N. Dharmaraj, P. Viswanathamurthi, K. Natarajan. *Transition Met. Chem.*, **26**, 105 (2001); (b) R. Malhotra, S. Kumar, K.S. Dhindsa. *Ind. J. Chem.*, **32A**, 457 (1993).
- [45] P.V. Anantha Lakshmi, P.S. Reddy, V.J. Raju. *Spectrochim Acta, Part A*, **74**, 52 (2009).
- [46] S. Bhushan, A. Kumar, F. Malik, S.S. Andotra, V.K. Sethi, I.P. Kaur, S.C. Taneja, G.N. Qazi, J.A. Singh. *Apoptosis*, **12**, 1911 (2007).